MODELING AND CFD SIMULATION OF THE DISPLACEMENT OF THE SOLID/LIQUID INTERFACE DURING CRYSTALLIZATION FOULING IN A GEOTHERMAL HEAT EXCHANGER

*** F. Cazenave, J. P. Serin, P. Bernada and F. Couture**
[*] Univ Pau & Pays Adour/ E2S UPPA, Laboratoire de Thermique, Energétique et Procédés- IPRA, EA1932, 64000, Pau, France, fl.cazenave@univ-pau.fr

ABSTRACT

Crystallization fouling in a geothermal heat exchanger is described by the modelling of mass, momentum and energy transport mechanisms. The multicomponent liquid flow includes ionic species, so electro-migration is taken into account in the transport model. A focus is made on the modelling of the moving interface between the fluid and the solid deposit, where the crystallization reaction occurs. A fully dynamic simulation of the model is conducted with spatial and temporal variations of the boundary condition on the temperature of the cold fluid of the heat exchanger. The growth by crystallization of the solid deposit over time and space is analyzed in terms of temperature, concentrations and fluid velocity.

INTRODUCTION

The occurrence of fouling in industrial devices often has severe consequences on their operation. In heat exchangers, this phenomenon creates an additional thermal resistance, which may cause an important decrease in heat flux [1]. Thus, the induced loss of thermal efficiency often leads to oversizing and large over-costs of heat exchangers [2]. Understanding the physicochemical and hydrodynamic mechanisms involved in the fouling phenomenon in the pipes seems to be key in order to define mitigation solutions.

Research on fouling and modelling attempts goes back to the beginning of the 20th century with a study published by Mc Cabe and Robinson [3]. The approach developed by Kern and Seaton [4] defined the solid growth as the result of a competition between a deposition and a removal rate. Many empirical deposition correlations were developed and used to calculate a fouling resistance and anticipate the impact of fouling on the operation of the heat exchanger and therefore improve sizing [5], [6]. The development of CFD has opened up new possibilities in the description of the fouling phenomenon. It allows a new approach, more precise, based on the modelling and simulation of mass, momentum and heat transport in the fluid flow. This gives access to the local fields of temperature, concentration, velocity and pressure along with the temporal and local thickness of the fouling layer. One of the first studies of crystallization fouling using CFD treated the calcium sulfate deposition as a fictitious crystal growth [7]. This mean that the impact of the solid formation is not taken into account in the hydrodynamics. This approach can also be found in other works such as Pääkkönen et al. [8] and Johnsen et al. [9]–[11]. Moreover, the diffusive term added to the kinetic law is redundant with the CFD description and not necessary. It is also relevant to notice that the kinetics used should be calculated from the local field of concentration and not mean values. Zhang et al. [12] presented a pseudo dynamic approach to improve the description, where they consider a succession of steady-state processes. This is an improvement but still not fully dynamic. It is also important to note that the models are very partially presented, including at the interface where the reaction occurs. To the best of our knowledge, the ionic character of the species involved is never taken into account; they are treated as uncharged.

This study focuses on the growth of a barite deposit by heterogeneous reaction on the surface of a cylindrical pipe. Barite has been identified as a salt susceptible of crystallizing in geothermal equipment [13]. The multicomponent transport model for the fluid and the conservation equations in both phases are described. The synthetic fluid is assumed to be composed of ions of barium and sulfate diluted in water. Since this study focuses on a surface crystallization reaction, the boundary conditions at the solid-liquid interface are detailed. A fully dynamic simulation of this model through CFD, using Comsol Multiphysics, is conducted. A spatial and temporal variation on the boundary condition on the external temperature is studied in order to demonstrate the abilities of the dynamic simulation.

DESCRIPTION OF THE MODELLING

Configuration

Crystallization fouling phenomenon by barite is studied in an AEL heat exchanger's pipe. The composition of the simplified brine consists in a ternary mixture of cations of barium (Ba^{2+}) and

ISBN: 978-0-9984188-1-0; Published online www.heatexchanger-fouling.com

anions of sulfate (SO_4^{2-}), diluted in water. As the liquid is flowing in the pipe of the heat exchanger, the temperature drops and can reach a value below the saturation point. A mono-constituent deposit is susceptible to form by crystallization according to the following reaction scheme:

$$Ba^{2+}_{(aq)} + SO^{2-}_{4\,(aq)} \rightarrow BaSO_{4(s)} \qquad (1)$$

In the following, Ba^{2+} and SO_4^{2-} are subscripted respectively "c" and "a". The subscript "w" is used to refer to the water. Barite is simply referred as "s". Variables in the liquid are subscripted "l", and "p" in the pipe.

The part of the pipe located after the entry box is considered. The steel pipe, the barite deposit and the fluid flow are the three domains modeled. The thermal behavior of the cold fluid is described thanks to a Dirichlet boundary condition. A thin deposit is assumed already present at the initial time and only the growth by crystallization is considered. An axisymmetric configuration is considered as shown in figure 1.

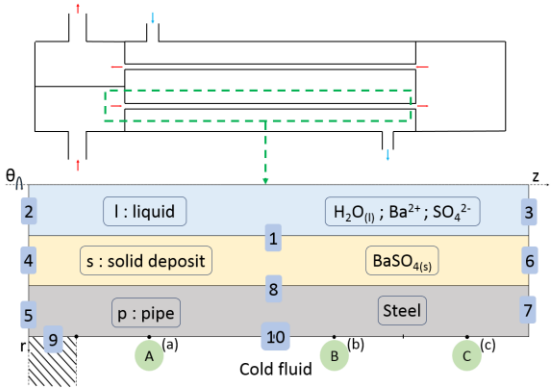

Fig 1 Schematic view of the configuration

Model

The presence of ionic species in the multicomponent liquid phase implies that transport by electro-migration needs to be accounted. The concentration of these charged species is very low [14]. Consequently, the fluid density is assimilated to the density of the water, which is assumed constant. Under this hypothesis, mass conservation equation with no homogeneous reactions reduces to volume conservation equation. In electrolytic solutions, it is classic to assume that electroneutrality is respected in the fluid, i.e. that negative charge balances exactly positive charge. It is also assumed that no electrical current is generated in the fluid, as it is the case in applications where only "ion exchange" occurs [15]. Thus, the current intensity vector is equal to zero. Momentum conservation is expressed by Navier-Stokes equation and an expression of the non-convective flux of the ionic species. The constitutive equation given by Del Rio and Whitaker is used [16]. It describes both diffusion and electro-migration, which involves the electric potential gradient that we express in terms of the other variables of the problem using the electroneutrality condition. Finally, the non-convective flux can be expressed of the form of a generalized Fick's law. Energy conservation includes both convection and conduction terms.

The two solid phases, pipe and barite deposit, are assumed homogeneous, non-deformable and static. Under these assumptions, the conservation equations reduces to energy conservation with only conductive heat transport.

To close the mathematical description, initial values are given for all the relevant variables. In addition to the symmetry conditions on the axis, boundary conditions are required on the other boundaries of the geometry. On the inlet side, the velocity and composition of the fluid is defined, and all three boundaries are set at the hot fluid temperature (2, 4 and 5 on figure 1). At the outlet, a fully established regime is assumed, so the normal gradient of the variables is equal to zero (3, 6 and 7 on figure 1). Pressure is specified at the liquid outlet. At the interface between the pipe and the deposit (8 on figure 1), we write heat flux continuity and thermal equilibrium. As said previously, a Dirichlet condition on the temperature is used, between the cold fluid and the pipe (10 on figure 1). In the heat exchanger, a wall separates the entry box for the hot fluid from the shell where the cold fluid flows (9 on figure 1). To account for the thermal behavior inside this wall, a linear profile between the two extreme temperatures is imposed. Finally, the liquid-deposit interface needs to be treated. This is the core of the study, as it is the interface where the crystallization reaction happens. This is why special attention is given to its description and the next paragraph is dedicated to it.

Solid-Liquid interface

The heterogeneous reaction takes place at the solid-liquid interface. The expression of the boundary conditions starts with the mass fluxes. The jump mass balance for the solid, traducing its growth (or dissolution) at the interface Σ, is given by

$$\rho_s \boldsymbol{w} \cdot \boldsymbol{n}_l = -r_s^{\Sigma} \qquad (2)$$

where $\boldsymbol{w}$ is the velocity of the interface Σ and r_s^{Σ} the mass rate of barite production. The liquid flux through the interface can be expressed in a similar way as

$$\rho_{li}(\boldsymbol{v}_{li} - \boldsymbol{w}) \cdot \boldsymbol{n}_l = -r_{li}^{\Sigma} \qquad \text{i=c,a,w} \qquad (3)$$

Here, r_{li}^{Σ} is the mass rate per unit area of production of species i by heterogeneous reaction. As the water is not involved in the reaction, it has no flux through the interface so its mass rate r_{lw}^{Σ} is equal to zero. According to the reaction equation (1), the

ISBN: 978-0-9984188-1-0; Published online www.heatexchanger-fouling.com

mass rates of reaction of the ionic species can be linked to the one of solid formation as

$$r_{li}^{\Sigma} = -\frac{M_{li}}{M_s} r_s^{\Sigma} \qquad \text{i=c,a} \tag{4}$$

To get a complete description, the mass rate of solid formation needs to be expressed. Under the assumption of an ideal solution, justified with diluted ionic species, a kinetic equation adapted from Zhen-Wu et al. [17] is used:

$$r_s^{\Sigma} = k_r \left(\frac{1}{M_c M_a} \frac{\rho_{lc}\rho_{la}}{C_s^{sat}(T^{\Sigma})^2} - 1 \right) M_s \tag{5}$$

In this equation, k_r designates the kinetic constant per unit area and $C_s^{sat}(T^{\Sigma})$ the molar saturation concentration at the interface temperature. The postulate that no mass can be created nor destroyed at the interface is verified [18]. It leads to:

$$r_{lc}^{\Sigma} + r_{la}^{\Sigma} + r_s^{\Sigma} = 0 \tag{6}$$

Using the expressions of the reaction rates (2, 3) in this previous equation and applying the definition of the mass-averaged velocity of the liquid phase, the normal velocity at the interface expresses as:

$$\boldsymbol{v}_l \cdot \boldsymbol{n}_l = \boldsymbol{w} \cdot \boldsymbol{n}_l \left(1 - \frac{\rho_s}{\rho_l} \right) \tag{7}$$

An expression for the tangential velocity is given by the no-slip condition:

$$\boldsymbol{v}_l . \boldsymbol{t}_l = 0 \tag{8}$$

The energy conservation equations at the interface requires two boundary conditions. First, thermal equilibrium is assumed:

$$T_l = T_s \tag{9}$$

Heat flux continuity at the interface involves the conductive fluxes $\boldsymbol{q}$ and the enthalpy of crystallization $\Delta_c h_s$ as:

$$r_s^{\Sigma} \Delta_c h_s + \boldsymbol{q}_l \cdot \boldsymbol{n}_l + \boldsymbol{q}_s \cdot \boldsymbol{n}_s = 0 \tag{10}$$

The next paragraph focuses on the numerical resolution of this model.

SIMULATION

Parameters values

A 2D axisymmetric configuration of a 2m pipe is considered. The inner radius of the pipe is 9.5 mm and it is 3 mm thick. The deposit initially present is 1 mm thick. The fluid enters at 90 °C and a laminar flow is considered with a uniform velocity of 0.1 $m.s^{-1}$ set at the inlet. The mass concentration of barium is $2.75x10^{-3}$ $kg.m^{-3}$ and $1.92x10^{-3}$ $kg.m^{-3}$ for sulfate ions. The pressure at the outlet is 20 bar.

The main parameters used for the simulation are given in table 1. The barite solubility value, at 20 bars, is correlated from experimental data published by Blount [19]

$$C_s^{sat}(T) = 3{,}8.10^{-9}T^3 - 2{,}2.10^{-6}T^2 + 3{,}1.10^{-4}T + 3{,}9.10^{-3} \tag{11}$$

where T is given in degree Celsius and C_s^{sat}, the solubility of the salt, in mole per cubic meter.

Similarly to density, the other fluid properties are assimilated to those of pure water and assumed constant. The available literature data at 25°C are taken for the fluid and solid properties (density, fluid viscosity, thermal conductivity and heat capacity). Properties for the pipe are taken from the Comsol library for AISI 4340 steel. The temperature dependency of the kinetic coefficient k_r is not available in the literature. Thus, we selected the value and the kinetic law formalism given by Zhen-Wu et al. [17].

Table 1. Simulation parameters, at 25 °C diluted in water

Parameter	Value	Unit
k_r [17]	$3.49x10^{-9}$	$mol.m^{-2}.s^{-1}$
D_1 [20]	$0.847x10^{-9}$	$m^2.s^{-1}$
D_2 [20]	$1.065x10^{-9}$	$m^2.s^{-1}$
$\Delta_c h_s$	111.4	$kJ.kg^{-1}$

Meshing

Free triangles are used to mesh the domain, with a boundary layer refinement on the fluid side, at the fluid-solid interface. It allows the nodes displacement without degenerating the triangles. ALE (Arbitrary Lagrangian Eulerian) method is used to handle the movement of the interface.

Simulation scenario

A fully dynamic simulation is conducted over a period of one year using Comsol Multiphysics. In order to test its abilities, spatial and temporal variations of the boundary condition on the cold fluid temperature are carried out. The cold fluid on the shell side of the heat exchanger is boiling. During the boiling process, the dry out phenomenon can happen. It traduces by the total evaporation of the liquid film on the heat transfer surface and thus by a sudden increase in surface temperature [21].

In order to emulate this behavior, two areas are considered, one where the thin liquid film is present at the surface of the pipe where the ebullition occurs and the other one where the liquid film has disappeared. As this fluid is not modelled, this phenomenon is expressed in terms of temperature, used as an exterior boundary condition on the pipe

ISBN: 978-0-9984188-1-0; Published online www.heatexchanger-fouling.com

(boundary 10 on figure 1). This boundary is divided in three areas noted (a), (b) and (c), respectively located at z between 0.003 and 1 meter, 1 to 1.5 meters and 1.5 to 2 meters. A temperature of 30 °C is set as a boundary condition for the first area (a). Therefore the boundary condition corresponding to the inside of the wall separating the shell from the entry box of the exchanger (9 on figure 1) is described by a linear profile going from 90 °C to 30°C. For part (c), a temperature of 60 °C is set. A sudden change of the conditions is investigated. It is represented here by a displacement of the area where the thin liquid film is present. A step function is created for the temperature of area (b) located in the middle of the boundary 10. It goes from 30 °C initially and increases rapidly to 60 °C at six month. The temperature conditions can be visualized on figure 2.

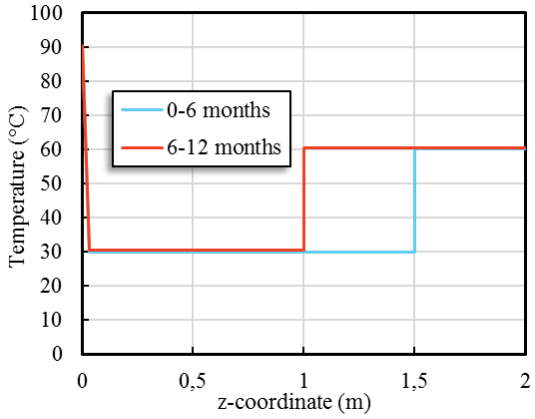

Fig 2 External temperature conditions on boundaries 9 and 10 over time

Results

A laminar boundary layer profile is simply verified for the hydrodynamics in the pipe, which are therefore not represented.

Three points of interest are defined, corresponding to the center of the three different areas of boundary 10. Point A is defined at z equal to 0.5 meter, B at 1.25 meters and C at 1.75 meters.

The effect of the changes made on the conditions on boundary 10 can be analyzed on figure 3, which represents the cross section of the temperature in the pipe. The plot is made at three z values corresponding to points A, B and C. For boundary (b), the values at two times are given before and after the evolution of the external temperature value. A significant change in the temperature profile can be observed. We also note that the conductive profile is linear in the pipe and the deposit. The temperature drops from about 5 to 10 K inside the deposit. This strong isolation effect leads to a loss of efficiency of the heat exchanger. Inside the fluid, the distribution is not uniform as a thermal boundary layer is developed. The mean temperature in the middle of the pipe decreases as expected along its length, regardless of the change of boundary condition.

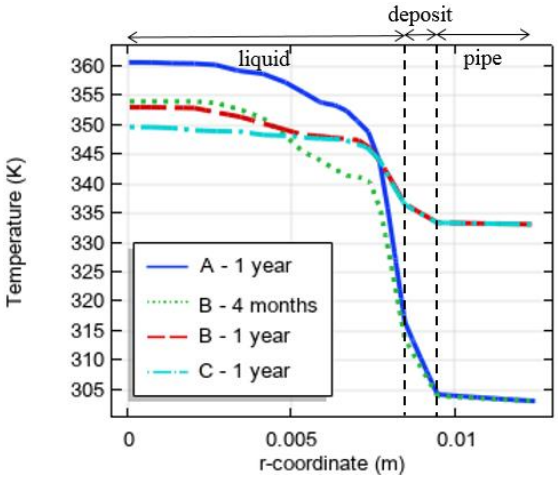

Fig 3 Cross section of the temperature for the three different types of boundaries conditions

The local and temporal evolution of the deposit can be analyzed on the whole length of the interface. First, we consider the evolution of the deposit thickness on the three points A, B and C.

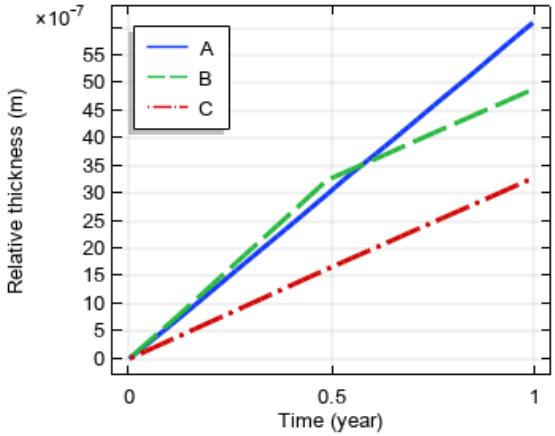

Fig 4 Temporal evolution of the relative thickness of the deposit at three points

The first thing that can be analyzed on figure 4 is that the solid is growing faster when the external temperature is 30 °C (area (a)) than 60 °C (area (c)). This difference of growth rate also leads to a change of slope at 6 month for the area (b), the growth velocity decreasing. As the evolution is linear for the two other areas ((a) and (c)), this change of slope can be explained by the increase of the external temperature to 60°C at six months.

ISBN: 978-0-9984188-1-0; Published online www.heatexchanger-fouling.com

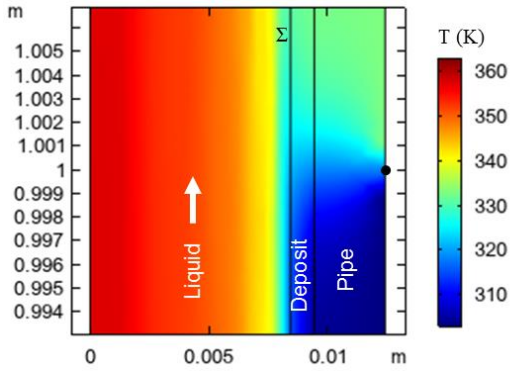

Fig 5 2D temperature profile in the middle of the pipe (t=1 year)

The temperature profile displayed on figure 5 confirms that the temperature of the interface is lower on the entrance side. The saturation concentration $C_s^{sat}(T^{\Sigma})$ is evolving in the same way than the temperature and this parameter is on the denominator of the kinetic law (5) which has a constant kinetic coefficient. Therefore, the reaction rate, which is directly linked to the interface velocity and thus the thickness of the deposit, tend to be higher over the area (a) of boundary 10. This confirms the observation made on figure 4. Nevertheless, there is an opposing effect of the species concentrations. Indeed, figure 6 shows that the concentration of barium is higher at point C than point A, so according to the kinetic equation, the reaction rate should evolve in the same way. This effect opposes to the previous one but is not preponderant. The thermal evolution of the surface of the deposit is the one affecting the solid growth.

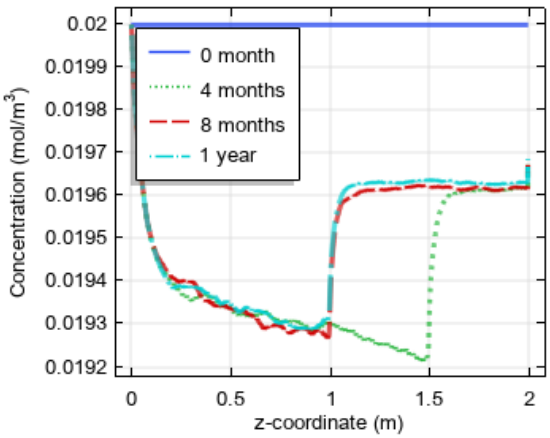

Fig 6 Concentration profiles of barium over the interface at different times

The temperature profile over the interface (figure 7) is very similar to the concentration profiles of figure 6. We note that this temperature of the interface is influenced by the external temperatures set on boundary 10 (figure 2).

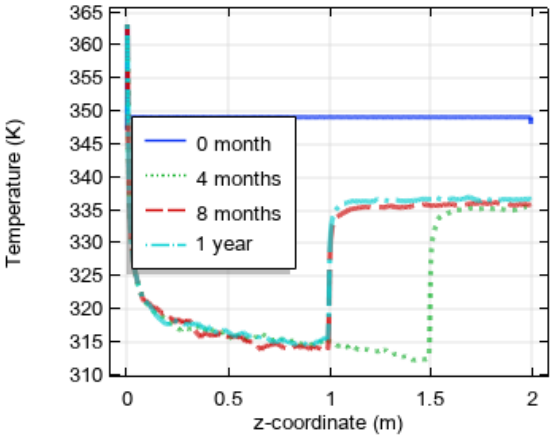

Fig 7 Temperature profile over the interface at different times

The difference of growth rate between points A and B up to six months displayed on figure 4 is confirmed by the shape of the deposit on figure 8. After six months however, the difference of growth rate reverses due to the sudden change of boundary condition.

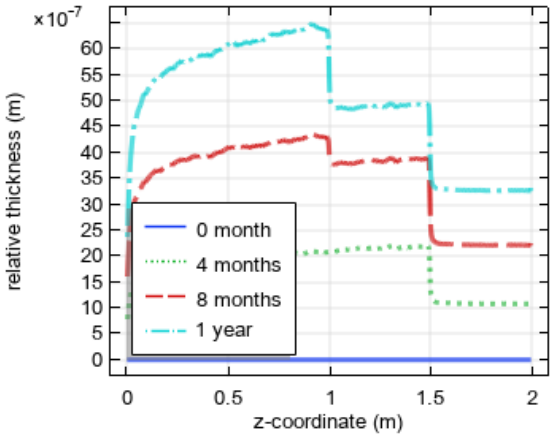

Fig 8 Spatial evolution of the relative thickness of the deposit at different times

CONCLUSION

The growth of a barite solid deposit in the pipe of a heat exchanger from a multicomponent fluid formed of barium and sulfate ions diluted in water is studied. The model is expressed at the continuum mechanics scale. The conservation equations are not detailed in this paper, but the description is complete for the solid-liquid interface where the heterogeneous reaction occurs. The modelling takes into account electro-migration, as ionic species are present.

The numerical resolution, conducted with Comsol Multiphysics, gives access to the spatial and temporal thickness of the deposit. The variation of the temperature of the cold fluid as a boundary condition demonstrates the interest of a fully dynamic simulation. The obtained profiles of

ISBN: 978-0-9984188-1-0; Published online www.heatexchanger-fouling.com

reaction rate and deposit shape can be interpreted by the local curves of temperature and concentration. The analysis also points out that the thermal behavior of the surface of the deposit has a preponderant effect on the reaction rate, rather than the concentrations values.

This model is able to predict the fouling behavior of geothermal equipment, including with dynamic fluctuations of the external working conditions. Nevertheless, taking into account industrial conditions would require a more complex description of the hot fluid, including more species and multiple crystallization reactions.

NOMENCLATURE

C^{sat}	Saturation concentration, mol.m^{-3}
D_i	Diffusion coefficient, m^2.s^{-1}
k_r	Kinetic constant, mol.m^{-2}.s^{-1}
M_i	Molar weight, kg.mol^{-1}
$\boldsymbol{n}$	Normal vector, dimensionless
$\boldsymbol{q}$	Conductive heat flux, W.m^{-2}
r_i	Mass rate of reaction per unit area of component i, kg.m^{-2}.s^{-1}
r, z, θ	Cylindrical coordinates, dimensionless
$\boldsymbol{t}$	Tangent vector
$\boldsymbol{v}_i$	Velocity of component i, m.s^{-1}
$\boldsymbol{v}$	Mass-averaged velocity, m.s^{-1}
$\boldsymbol{w}$	Velocity of the interface, m.s^{-1}
T	Temperature, K
$\Delta_c h_s$	Enthalpy of crystallization, kJ.kg^{-1}
ρ	Total mass density of the phase, kg.m^{-3}
ρ_i	Mass concentration of species i, kg.m^{-3}
Σ	Liquid-deposit interface, dimensionless

Subscript

l	Liquid
s	Solid
1	Barium ions
2	Sulfate ions
3	Water

REFERENCES

[1] D. Hasson, « Rate of decrease of heat transfer due to scale deposition », *Dechema-Monogr.*, vol. 47, p. 233–252, 1962.

[2] T. R. Galloway, « Heat transfer fouling through growth of calcareous film deposits », *Int. J. Heat Mass Transf.*, vol. 16, nº 2, p. 443–458, 1973.

[3] W. L. McCabe et C. S. Robinson, « Evaporator scale formation », *Ind. Eng. Chem.*, vol. 16, nº 5, p. 478–479, 1924.

[4] D. Q. Kern et R. E. Seaton, « A theoretical analysis of thermal surface fouling », *Br. Chem. Eng.*, vol. 4, nº 5, p. 258–262, 1959.

[5] S. Krause, « Fouling of heat-transfer surfaces by crystallization and sedimentation », *Int. Chem. Eng. Q. J. Transl. Russ. East. Eur. AsiaUnited States*, vol. 33, nº 3, 1993.

[6] H. Müller-Steinhagen, « Heat transfer fouling: 50 years after the Kern and Seaton model », *Heat Transf. Eng.*, vol. 32, nº 1, p. 1–13, 2011.

[7] F. Brahim, W. Augustin, et M. Bohnet, « Numerical simulation of the fouling process », *Int. J. Therm. Sci.*, vol. 42, nº 3, p. 323–334, 2003.

[8] T. M. Pääkkönen *et al.*, « CFD modelling of CaCO 3 crystallization fouling on heat transfer surfaces », *Int. J. Heat Mass Transf.*, vol. 97, p. 618–630, 2016.

[9] S. G. Johnsen, S. T. Johansen, et B. Wittgens, « A wall-function approach for direct precipitation/crystallization fouling in CFD modelling », *ArXiv170602931 Phys.*, 2017.

[10] S. G. Johnsen, T. M. Pääkkönen, S. T. Johansen, R. L. Keiski, et B. Wittgens, « Implementation, demonstration and validation of a user-defined wall-function for direct precipitation fouling in ANSYS Fluent », *ArXiv170601453 Cs*, 2017.

[11] S. G. Johnsen, T. M. Pääkkönen, S. Andersson, S. T. Johansen, et B. Wittgens, « On the wall boundary conditions for species-specific mass conservation equations in mathematical modelling of direct precipitation fouling from supersaturated, multi-component fluid mixtures », *ArXiv170301448 Phys.*, 2017.

[12] F. Zhang, J. Xiao, et X. D. Chen, « Towards predictive modeling of crystallization fouling: A pseudo-dynamic approach », *Food Bioprod. Process.*, vol. 93, p. 188–196, 2015.

[13] E. Bozau, S. Häußler, et W. van Berk, « Hydrogeochemical modelling of corrosion effects and barite scaling in deep geothermal wells of the North German Basin using PHREEQC and PHAST », *Geothermics*, vol. 53, p. 540‑547, janv. 2015.

[14] B. Sanjuan, R. Millot, C. Dezayes, et M. Brach, « Main characteristics of the deep geothermal brine (5km) at Soultz-sous-Forêts (France) determined using geochemical and tracer test data », *Comptes Rendus Geosci.*, vol. 342, nº 7, p. 546‑559, juill. 2010.

[15] R. Taylor et R. Krishna, *Multicomponent Mass Transfer*. John Wiley & Sons, 1993.

[16] J. A. del Río et S. Whitaker, « Diffusion of Charged Species in Liquids », *Sci. Rep.*, vol. 6, 2016.

[17] B. Y. Zhen-Wu, K. Dideriksen, J. Olsson, P. J. Raahauge, S. L. S. Stipp, et E. H. Oelkers, « Experimental determination of barite dissolution and precipitation rates as a function of temperature and aqueous fluid composition », *Geochim. Cosmochim. Acta*, vol. 194, p. 193‑210, 2016.

[18] C. Truesdell, « Thermodynamics of Diffusion », in *Rational Thermodynamics*, C.

ISBN: 978-0-9984188-1-0; Published online www.heatexchanger-fouling.com

Truesdell, Éd. New York, NY: Springer New York, 1984, p. 219‑236.
[19] C. W. Blount, « Barite solubilities and thermodynamic quantities up to 300/sup 0/C and 1400 bars », *Am Miner. U. S.*, vol. 62:9‑10, 1976.
[20] Lide, *CRC Handbook of Chemistry and Physics*. CRC Press, New York, 2005.
[21] M. S. Kamel, F. Lezsovits, A. M. Hussein, O. Mahian, et S. Wongwises, « Latest developments in boiling critical heat flux using nanofluids: A concise review », *Int. Commun. Heat Mass Transf.*, vol. 98, p. 59‑66, nov. 2018.

ISBN: 978-0-9984188-1-0; Published online www.heatexchanger-fouling.com